energies

MDPI

Article

Screening of Nickel and Platinum Catalysts for Glycerol Conversion to Gas Products in Hydrothermal Media

Carine T. Alves [1,2] and Jude A. Onwudili [1,*]

[1] Energy and Bioproducts Research Institute, School of Infrastructure and Sustainable Engineering, College of Engineering and Physical Sciences, Aston University, Birmingham B4 7ET, UK
[2] Energy Engineering Department, Universidade Federal do Reconcavo da Bahia, Av. Centenario 697, Feira de Santana 44085-132, Brazil
* Correspondence: j.onwudili@aston.ac.uk

Abstract: The production of low-carbon gaseous fuels from biomass has the potential to reduce greenhouse gas emissions and promote energy sustainability, stability and affordability around the world. Glycerol, a large-volume by-product of biodiesel production, is a potential feedstock for the production of low-carbon energy vectors. In this present work, an aqueous solution of pure glycerol was reacted under hydrothermal conditions using a total of 10 types of heterogeneous catalysts to evaluate its conversion to gas products (hydrogen, methane, CO, CO_2 and C_2–C_4 hydrocarbon gases). Two bimetallic Ni-Fe and Ni-Cu catalysts, three Pt-based catalysts and physical mixtures of the five catalysts were tested. The reactions were carried out in a batch reactor for 1 h reaction time, using a 9:1 mass ratio of water/glycerol (10 wt%) and the reaction temperatures ranged between 250–350 °C using and without using 1 g of catalyst. The effects of the catalysts and reaction conditions on the conversion of glycerol in terms of carbon and hydrogen gasification efficiencies, selectivity and yields of components in the gas products were investigated. CO_2 remained the most dominant gas product in all experiments. The results indicated that increasing the reaction temperature favoured gas formation and both carbon and hydrogen gasification efficiencies. The combination of Ni-Cu and Pt/C catalysts was the most selective catalyst for gas formation at 350 °C, giving carbon gasification efficiency of 95.6 wt%. Individually, the catalyst with the highest hydrogen production was Pt/C and the highest propane yield was obtained with the Ni-Cu bimetallic catalyst. Some catalysts showed good structural stability in hydrothermal media but need improvements towards better yields of desired fuel gases.

Keywords: hydrothermal reforming; glycerol; hydrogen; propane; heterogeneous catalysis

Citation: Alves, C.T.; Onwudili, J.A. Screening of Nickel and Platinum Catalysts for Glycerol Conversion to Gas Products in Hydrothermal Media. *Energies* **2022**, *15*, 7571. https://doi.org/10.3390/en15207571

Academic Editors: Xiaohan Ren, Fei Sun and Juan Chen

Received: 9 September 2022
Accepted: 7 October 2022
Published: 13 October 2022

1. Introduction

Currently, several research groups around the world are studying different ways to efficiently use available biomass resources to contribute to the production of new energy sources, chemical intermediates and to reduce CO_2 emissions from fossil sources [1–4]. First generation biofuels and chemicals are produced using derivatives of sugars and vegetable oils. Presently, many technological routes are being studied to valorise lignocellulosic residues to obtain products with high added value, such as chemical products, liquids, and gaseous fuels.

With the main objective of avoiding any conflict in the food chain, currently the production of biodiesel from non-edible and waste lipids is being developed in biorefineries. Biodiesel is mainly produced from the reaction (esterification and transesterification) of fatty acids, vegetable oil and lipids with an alcohol (mainly, methanol) in the presence of an alkaline catalyst. Glycerol (glycerin or 1,2,3-propanetriol) is the main by-product of biodiesel production from triglycerides. For every 100 kg of biodiesel made, about 10 kg of crude glycerol is produced [5]. The global biodiesel market was valued at US

$32.09 billion in 2021 and is expected to grow at a growth rate of 10% from 2022 to 2030 in line with the forecasts of a significant increase in biodiesel production, as part of a successful biorefinery concept [6]. The increase in biodiesel production will contribute to an excess of crude glycerol, making it available as a relatively low-cost feedstock for chemical transformation [7].

The conversion of glycerol to gaseous fuels such as hydrogen, methane and propane is an important research area [8]. The major constituents of the compounds formed in the thermal (non-catalytic) decomposition of glycerol have been reported to be carbon monoxide, hydrogen and carbon dioxide [9]. Other compounds obtained from this process included methanol, ethanol, methane ethylene, acetaldehyde, acetic acid, acetone, acrolein and water [9]. Therefore, there may be a need to explore the use of catalysts to alter the selectivity of the reaction products towards fuel gases.

The VIII group metals have been extensively used in glycerol reforming reactions, and Pt is highly active for C–C cleavage, as well as water gas shift (WGS) reactions [10]. While Ni offers a cheaper alternative to Pt, its high methanation activity involves hydrogen consumption, which is not beneficial if the process targets hydrogen as the main gaseous fuel [11]. However, the selectivity of catalysts can be improved by the use of a bimetallic catalyst or doping of the active metal [8]. Furthermore, appropriate catalyst supports used to disperse the active metals may provide additional selectivity benefits through metal-support interaction or by providing co-catalytic active sites during the reforming. The most used catalyst supports for hydrothermal reforming reactions are alumina and carbon [12]. Seretis and Tsiakaras [13] investigated the effect of operational conditions on glycerol reforming in a batch reactor using 5 wt% Pt/Al_2O_3 as a catalyst. Longer reaction times of up to 4 h lead to a decrease in hydrogen yield at 200 °C, which demonstrated the promotion of methanation and hydrogenation to produce alcohols and alkanes [13]. Shabaker et al. [14] reported that hydrogen selectivity decreased when the temperature was increased to around 265 °C in the presence of 3 wt% Pt/Al_2O_3, which they attributed to the increased formation of CO_2 and CH_4 at higher glycerol conversion (50–99%). Their work also showed that increased methane yield indicated hydrogen consumption to produce methane [14]. Therefore, the literature showed that the conversion of glycerol to gaseous products increased when time and temperature were raised but with poor selectivity towards hydrogen [13,14].

Platinum and other noble metals are known to have activity towards C-H bond cleavage, but their high cost and limited availability often reduce their use as catalysts [15]. In contrast, non-noble transition metal catalysts like Ni are readily available, not expensive and can be equally active during certain reactions. Ni-based catalysts are commonly used in reforming reactions, as they display good intrinsic activity and can achieve good dispersion over support materials [16,17]. However, the presence of this catalyst can promote the production of CO and methane under certain reforming reactions, while also promoting H_2 production in certain cases [18,19]. Nevertheless, the ease of deactivation via coking and sintering of metal clusters remains a major challenge for Ni-based catalysts [20]. Hence, there is a current focus to design new catalysts which combine different synergistic metals and supports to achieve high selectivity towards the desirable gas products and good catalyst stability at reduced costs. However, most research efforts in this area are around steam reforming of glycerol [21].

Touri and Taghizadeh [22] synthesized Pt/SiO_2 nano-catalyst by sol-gel method for steam reforming of glycerol (SRG) at a temperature range of 300–400 °C and atmospheric pressure in a micro-channel reactor. By evaluating the catalyst performance through glycerol conversion, hydrogen yield and the selectivity of the exit gas, the authors achieved optimum conditions at an inlet feed flow rate of 3 mL/h and temperature of 400 °C, which gave high hydrogen yield of 89.7% and a low selectivity towards CO [22].

Chakinala and Chakinala [23] reported hydrogen production from hydrothermal reforming of glycerol using different types of active metals on alumina support and palladium with different supports at 450 °C and 250 bar to 6 h duration. The maximum carbon gasifi-

cation efficiency of 70% and hydrogen yield of 2.023 mol/mol was shown using platinum and the lowest of ~7.5 was achieved using a Ni-based catalyst with low hydrogen yields of 0.021 mol/mol. With different supports, the maximum carbon gasification efficiency of ~65% and hydrogen yield of 2.475 mol/mol were obtained with ceria-modified zirconia support [23].

Aqueous-phase reforming of glycerol has been reported in the literature but mostly with a focus on producing one type of fuel gas. For example, platinum-based catalysts have been reported as effective for APR of glycerol for hydrogen production [24,25]. In addition, methane production has also been reported during APR of glycerol using nickel-based catalysts [26], by promoting hydrogen production for in-situ hydrogenation of CO and CO_2 to methane.

This present study explores the possibility of producing three fuel gases, namely hydrogen, methane and propane from APR of glycerol, through the screening of nickel-based, catalysts, platinum-based catalysts and their combinations. The development of bimetallic (i.e., Pt-Ni and Cu-Ni) catalysts has been found to be a good solution towards these problems [16,17]. This present study has focused on the screening of Ni-based and Pt-based catalysts for the hydrothermal reforming of glycerol using different formulations of these catalysts to produce gaseous biofuels. The reactions involved the use of bimetallic $NiFe_2O_4$ and Ni-Cu/Al_2O_3 and mono metallic Pt catalysts (Pt/C, Pt/SiO_2 and Pt/Al_2O_3) as well as the combinations of each of the Ni-based catalysts with the Pt catalysts to give a total of 10 catalyst systems to test. The glycerol reforming reactions were carried out in a batch reactor from 250–350 °C, followed by a detailed analysis of the gas products and used catalysts. The results would be used to explain the effect of these catalysts on glycerol reforming to improve the selectivity of hydrogen, methane, or propane. To follow the main reforming reactions, pure glycerol has been used in this study to avoid any challenges arising from impurities from crude glycerol.

2. Materials and Methods

2.1. Materials

Pure glycerol (+99%) feedstock and 5 wt% platinum on carbon support (Pt/C) catalyst were purchased from Fisher Scientific, Leicester, UK. The Ni-Cu/Al_2O_3, (10 wt% each metal), 5 wt% Pt/SiO_2 and 5 wt% Pt/Al_2O_3 were obtained from Catal International Limited, Sheffield, UK. $NiFe_2O_4$ was synthesised by the combustion method as reported in previous work [27]. All catalysts were obtained in their reduced form and used as received. Deionised water was obtained in-house from a Milli-Q Advantage A10 Water Purification System.

2.2. Experimental Methods

2.2.1. Characterisation of Feedstock and Catalysts

A Flash 2000 Elemental analyser was used to quantify the amount of carbon, hydrogen, nitrogen, sulphur, and oxygen (calculated by difference). The elemental compositions and higher heating value (Equation (1)) of the pure glycerol are shown in Table 1.

$$\text{Dulong's formula: HHV (MJ/kg)} = 0.3383C + 1.443(H - (O/8)) + 0.0942S \quad (1)$$

where C, H, O and S are the wt% composition of carbon, hydrogen, oxygen and sulphur, respectively.

Table 1. Elemental analysis of glycerol.

Sample	C (wt%)	H (%)	N (%)	S (%)	O (%)	HHV (MJ/kg)	Density at 20 °C (kg/m^3)	Ash (wt%)	Moisture (wt%)
Glycerol	40.8 ± 0.43	9.86 ± 0.20	0.12 ± 0.01	nd	49.3 ± 0.62	19.1 ± 0.54	1261.3 ± 0.00	nd	0.11 ± 0.03

nd: not detected.

A Bruker D8 Advance diffractometer using Cu Kα1,2 radiation (40 mA and 40 kV, 0.02 mm Ni Kβ filter and 2.5° Soller slits, scanning from 5 to 105°) was used for X-ray diffraction (XRD) analysis of the fresh and recovered catalysts. The fresh and recovered catalysts were top-loaded into PMMA specimen holders and the diffractograms were collected in the Bragg–Brentano geometry with a step scan of 0.02° (1 s per step). Peaks on the diffractograms were assigned based on the International Centre for Diffraction Data's (ICDD) Powder Diffraction File-2 2012 (PDF-2 2012) and Inorganic Crystal Structure databases ICSD.

2.2.2. Experimental Set-Up

The experimental procedure for the hydrothermal reforming of glycerol experiments is presented in Figure 1. A 100 mL batch reactor was used to carry out the reactions with loadings of 2 g of glycerol, 18 g of deionised water (glycerol/water mass ratio of 1:9) and 1 g of catalyst (glycerol/catalyst mass ratio of 2:1). After loading the reactor with the required sample and amount of water, it was sealed and purged and thereafter pressurised with nitrogen to 5-bar.

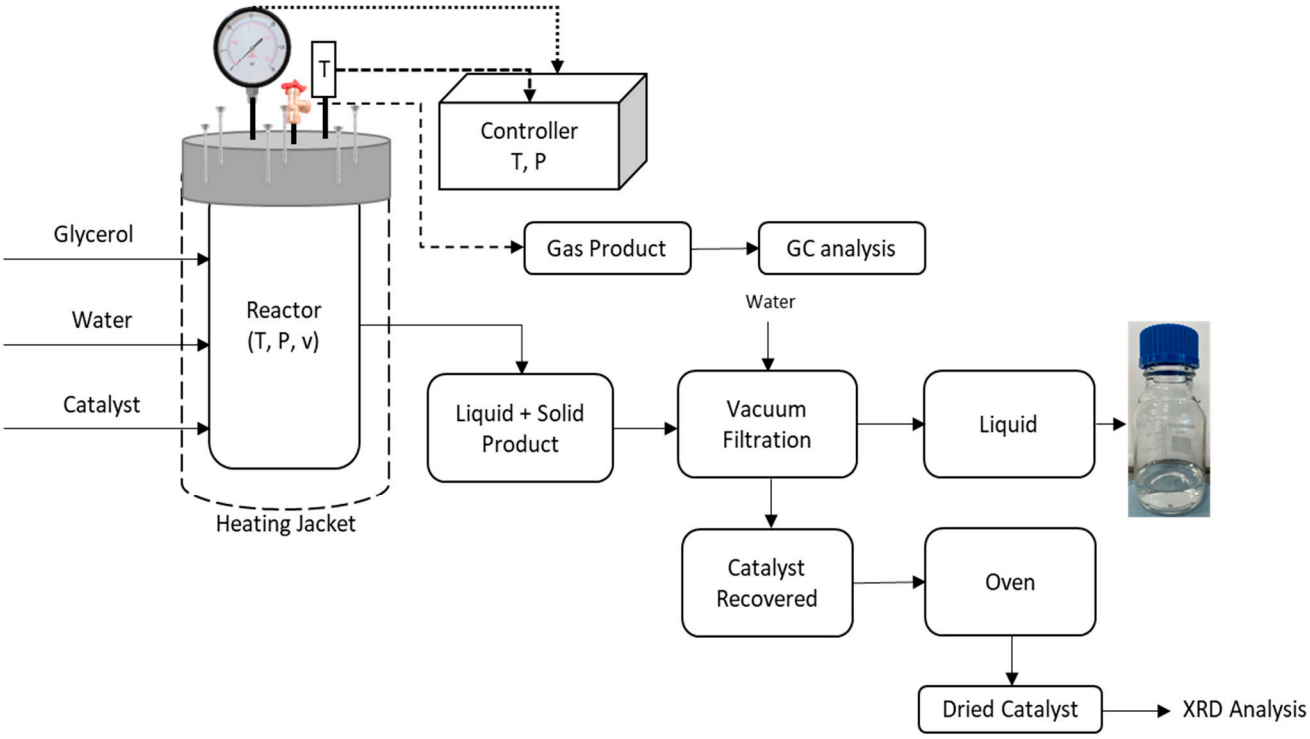

Figure 1. Schematic of the experimental procedure used in this study.

The reactor was externally heated with a heating jacket at an average rate of 7 °C/min until settled temperature (250 °C, 300 °C or 350 °C) and held for 60 min. At the end of the reaction, the reactor was removed from the heater and cooled to room temperature with a laboratory fan, taking about 30 min to reach ambient temperature. The gas formation after cooling was observed by the controller and the gaseous product was collected using a gas-bag and injected into a GC (Shimadzu GC-TCD/FID) for identification and quantification.

The reacted contents were quantitatively transferred into a 250 mL sample bottle using 40 mL of deionized water, to dissolve and recover the reaction products. Thereafter, the liquid and solid products (catalyst) were passed through vacuum filtration prior to being separated using a separating funnel and recovering the catalyst from the liquid sample. Each product was weighed separately for mass balance calculation. The recovered catalyst was dried at 105 °C for 2 h in a vacuum oven.

2.2.3. Analysis of Products

A simplified scheme for the analytical procedures used for the gaseous, liquid and solid reaction products are shown in Figure 2. The cooled product gas was collected from the reactor into the Tedlar bag by opening the gas outlet valve. Then, the liquid and solid (catalyst) products were collected after the head of the reactor was unscrewed and removed. The liquid and solid products were collected from the reactor by rinsing them with 40 mL of distilled water. All liquid and solid products (catalyst) were passed through vacuum filtration to separate and recover the catalyst. The number of recovered catalysts (~1 g) was confirmed to be unchanged following thermogravimetric analyses, with no significant mass losses observed. The fresh and recovered catalysts were analysed by XRD. The main focus of this work being were the gas products and catalysts, hence no liquid effluent was characterised, considering that 100% conversion of glycerol was achieved in some cases.

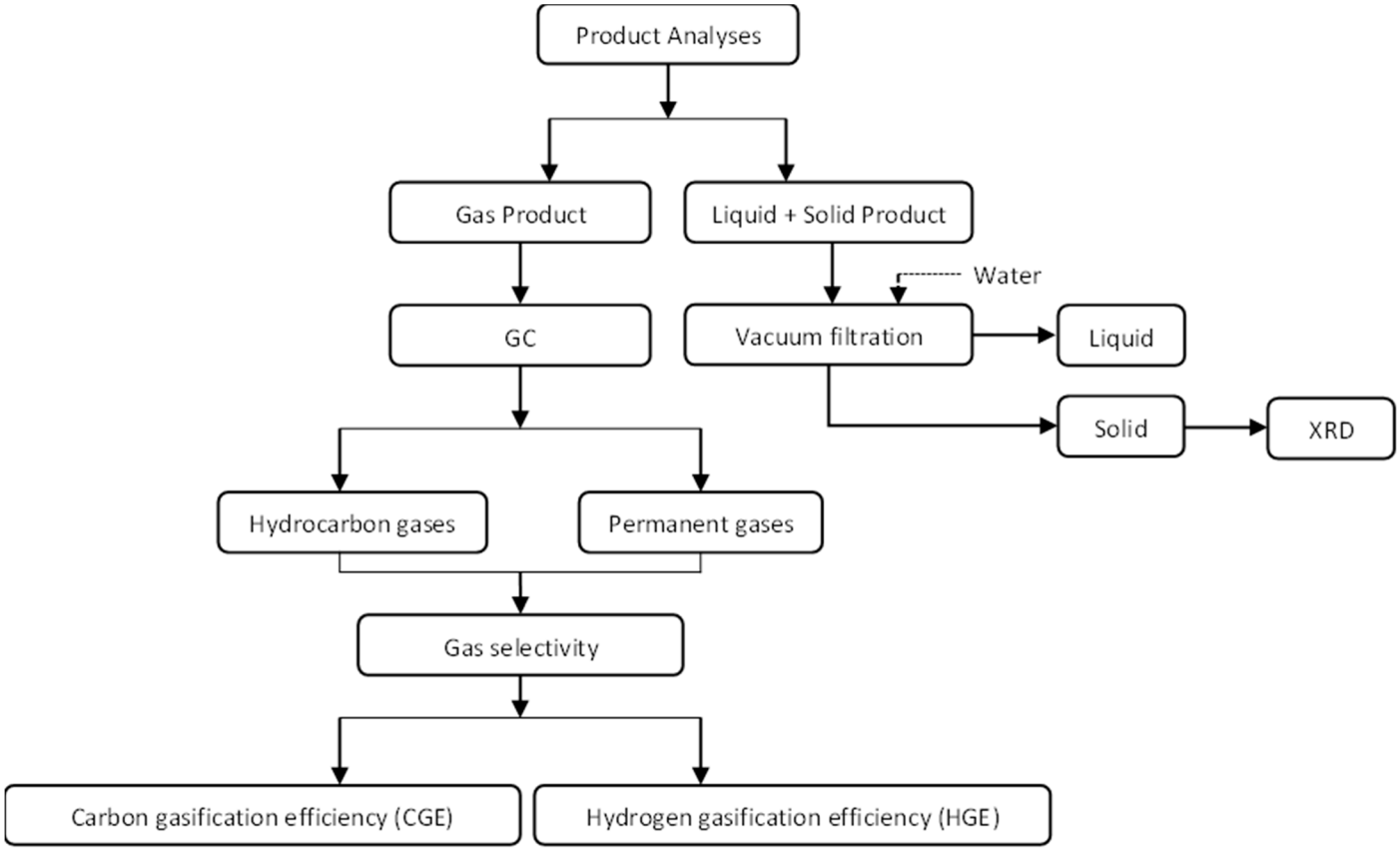

Figure 2. Schematic for product analyses.

Gas Product Analysis

The gas products were analysed according to the method described in a previous work [27]. Briefly, a Shimadzu GC-2014 gas chromatograph fitted with two injection ports and two detectors was used. The injectors and detectors were held at 60 °C and 220 °C, respectively. A thermal conductivity detector (TCD) held at was used to quantify the permanent gases (hydrogen, nitrogen, oxygen carbon dioxide and carbon monoxide), after separation on a 2 m length by 2 mm diameter 60–80 mesh molecular sieve column. However, the carbon dioxide was separated on a 2 mm diameter Hayesep 80–100 mesh column. In addition, a flame ionisation detector (FID) was used to quantify C_1–C_4 hydrocarbon gases, which were separated on another 2 m length by 2 mm diameter Hayesep 80–100 mesh column. A gas sample injection size of 0.6 mL was used for both the product gases and standards. Both columns were operated at the same temperature programme for a total of 13 min analysis time: start at 80 °C, ramped at 10 °C min^{-1} to 180 °C and then held at 180 °C.

2.3. Carbon and Hydrogen Gasification Efficiencies (CGE and HGE)

The yields of gas products were calculated using on General Gas Equation and evaluated according to Equations (2)–(4):

The molar composition of the gas product (x_i):

$$x_i\ (\%) = \frac{n_i}{n_{total}} \times 100 \quad (2)$$

Carbon gasification efficiency (*CGE*):

$$CGE\ (\%) = \frac{mass\ of\ carbon\ in\ gas\ products}{mass\ of\ carbon\ in\ feed} \times 100 \quad (3)$$

Hydrogen gasification efficiency (*HGE*):

$$HGE\ (\%) = \frac{mass\ of\ hydrogen\ in\ gas\ products}{mass\ of\ hydrogen\ in\ feed} \times 100 \quad (4)$$

The mass of carbon and hydrogen in gaseous products were calculated based on each gas product mass (g) obtained from the GC based on carbon and hydrogen content, respectively. The mass of carbon and hydrogen in the feed was calculated based on the quantities of these components in the liquid phase (feed).

3. Results and Discussions

3.1. Conversion of Glycerol in Relation to Catalyst and Reaction Conditions

In this present study, to evaluate the influence of the bimetallic catalysts in the catalytic reforming of glycerol, the synthesised $NiFe_2O_4$ and the commercial Ni-Cu/Al_2O_3 catalysts were tested at 250 °C, 300 °C and 350 °C, 60 min of reaction time, using 10 wt% glycerol in water and 1 g of catalyst. It was found that the conversion of glycerol to gas was nearly complete at 350 °C and the gases at the reactor outlet contained CH_4, C_2–C_4, H_2, CO and CO_2. Pt-based fresh catalysts (5 wt% Pt/C, 5 wt% Pt/Al_2O_3 and 5 wt% Pt/SiO_2) were also tested at 350 °C (Table 2).

The results of each reaction test and the corresponding conversion are shown in Table 2, and they indicated that increasing the temperature with and without catalyst, favoured the conversion significantly. As it can be seen from Table 2, high conversions (>99%) were obtained from 5 wt% Pt/C (97.67%), Ni-Cu/Al_2O_3 + Pt/Al_2O_3 (99.67%), Ni-Cu/Al_2O_3 + Pt/C (99.73%), 5 wt% Pt/Al_2O_3 (99.84%) and $NiFe_2O_4$ + Pt/C (99.84%), while for $NiFe_2O_4$ + Pt/SiO_2, 5 wt% Pt/SiO_2 and Ni-Cu/Al_2O_3 + Pt/SiO_2 produced the lowest values of 27.51%, 32.53% and 35.83%, respectively at 350 °C for 60 min reaction time, using 10 wt% glycerol in water and 1 g of catalyst. As the two sets of catalysts contained the same amount and form of Pt, the large differences in results could only be due to their supports. It has been reported that carbon supports provide greater dispersion and stability in hydrothermal conditions compared to silica. [28,29]. In the absence of catalysts, the conversion increased with temperature and reached 41.90% at 350 °C, which was higher than those obtained from the Pt/SiO_2 catalyst at 350 °C.

Early results showed that the Ni-Cu/Al_2O_3 catalyst was promising and gave lower conversions and selectivities compared to Pt/C or Pt/Al_2O_3. Nickel-based catalysts are generally regarded as being cost-effective, and they are also known to promote the water-gas shift reaction and to largely suppress tar formation due to an enhanced ability for cracking organic compounds [30]. In particular, C–C cleavage in glycerol leads to the formation of shorter carbon chain molecules (e.g., ethylene glycol). In contrast, breaking the C-O bond usually uses hydrogen and leads to the formation of alkanes, whose reforming is thermodynamically prevented at the relatively low temperatures used in this type of reaction. The main objective of this work was to obtain high yields of low-carbon renewable fuel gases (hydrogen, methane and propane) by reducing the catalyst and energy costs of the catalytic reforming of glycerol. In addition, carbon monoxide is both a combustible gas and

can also undergo a water-gas reaction to produce hydrogen gas, therefore can be included in the hydrogen generation potential of reforming reactions. Given the low glycerol conversions with the Ni-based catalysts (Table 2, various physical mixtures of the Ni-based and Pt-based catalysts were tested. The Ni-Cu/Al_2O_3 catalyst was combined in 50/50 wt% with 5 wt% Pt/C, 5 wt% Pt/Al_2O_3 and 5 wt% Pt/SiO_2 in the same reaction conditions used for the individual catalysts. Table 2 shows that when combined with Ni-Cu/Al_2O_3, the Pt/SiO_2 still gave low conversion (38.83%) and in contrast, combining Ni-Cu/Al_2O_3 with Pt/Al_2O_3 and Pt/C and significantly increased to 99.67% and 99.73% at 350 °C, respectively. Conversion data indicated that by combining the Ni-Cu/Al_2O_3 with Pt-based catalysts in a 1:1 mass ratio, the Pt/C catalyst gave the best results (Pt/C > Pt/Al_2O_3 >>> Pt/SiO_2).

Table 2. Glycerol conversions under various catalytic hydrothermal reforming conditions.

Catalyst	*m* Glycerol (g)	*m* Water (g)	*m* Catalyst (g)	Time (min)	Temperature (°C)	Maximum Pressure (bar)	Conversion (%)
No Catalyst	2.07 ± 0.01	20	0.00	60	250	36.7 ± 0.0	0.48 ± 0.01
	2.08 ± 0.01	20	0.00	60	300	82.5 ± 0.1	0.94 ± 0.01
	2.05 ± 0.02	20	0.00	60	350	129.3 ± 0.1	41.90 ± 0.01
$NiFe_2O_4$	2.08 ± 0.03	20	1.01	60	250	37.3 ± 0.0	0.70 ± 0.00
	2.00 ± 0.03	20	1.02	60	300	86.8 ± 0.1	28.61 ± 0.01
	2.10 ± 0.00	20	1.02	60	350	130.5 ± 0.0	53.11 ± 0.02
Ni-Cu/Al_2O_3	2.05 ± 0.01	20	1.02	60	250	36.9 ± 0.1	1.10 ± 0.02
	2.10 ± 0.01	20	1.01	60	300	86.5 ± 0.3	14.24 ± 0.05
	1.98 ± 0.01	20	1.04	60	350	161.0 ± 0.0	63.45 ± 0.03
5 wt% Pt/SiO_2	2.08 ± 0.01	20	1.01	60	350	160.6 ± 0.1	32.53 ± 0.02
5 wt% Pt/Al_2O_3	2.08 ± 0.01	20	1.01	60	350	163.3 ± 0.1	99.84 ± 0.01
5 wt% Pt/C	2.07 ± 0.02	20	1.02	60	350	175.70 ± 0.1	97.67 ± 0.05
$NiFe_2O_4$ and 5 wt% Pt/SiO_2	2.09 ± 0.00	20	1.00	60	350	171.0 ± 0.1	27.51 ± 0.01
$NiFe_2O_4$ and 5 wt% Pt/Al_2O_3	2.04 ± 0.01	20	1.03	60	350	172.5 ± 0.3	32.92 ± 0.03
$NiFe_2O_4$ and 5 wt% Pt/C	2.08 ± 0.01	20	1.01	60	350	164.9 ± 0.2	99.84 ± 0.03
Ni-Cu/Al_2O_3 and 5 wt% Pt/SiO_2	2.04 ± 0.02	20	1.05	60	250	37.7 ± 0.0	3.52 ± 0.03
	2.05 ± 0.01	20	1.00	60	300	84.6 ± 0.2	8.62 ± 0.03
	2.04 ± 0.02	20	1.01	60	350	173.4 ± 0.1	35.83 ± 0.00
Ni-Cu/Al_2O_3 and 5 wt% Pt/Al_2O_3	2.10 ± 0.03	20	1.07	60	250	51.6 ± 0.1	23.52 ± 0.03
	2.05 ± 0.01	20	1.02	60	300	88.9 ± 0.0	29.44 ± 0.05
	2.04 ± 0.01	20	1.02	60	350	165.9 ± 0.1	99.67 ± 0.04
Ni-Cu/Al_2O_3 and 5 wt% Pt/C	2.03 ± 0.02	20	1.02	60	250	37.0 ± 0.0	21.22 ± 0.02
	2.05 ± 0.01	20	1.01	60	300	87.1 ± 0.1	42.59 ± 0.00
	2.05 ± 0.01	20	1.01	60	350	165.9 ± 0.1	99.73 ± 0.04

Also, the $NiFe_2O_4$ catalyst was tested combined with Pt-based catalysts (Pt/C, Pt/Al_2O_3 and Pt/SiO_2) at 350 °C and the results showed the same pathway (Pt/C > Pt/Al_2O_3 >>> Pt/SiO_2) than the Ni-Cu/Al_2O_3 combined with Pt-based catalysts, however, the gas conversion was lower as can be seen in Table 2. These results are in accordance with the fresh catalysts, with the nickel ferrite alone being less efficient than the Ni-Cu/Al_2O_3.

In fact, using Pt/Al_2O_3 alone resulted in similar glycerol conversion (99.84%) as combining this catalyst with Ni-Cu/Al_2O_3 (99.67%) but in much lower conversion when combined with $NiFe_2O_4$ (32.92%). Hence, it could be argued that some synergy existed between Ni-Cu/Al_2O_3 and Pt/Al_2O_3. Hence, by reducing the Pt-based catalysts by half, similar glycerol conversion was achieved (Table 2), which would help reduce catalyst costs, if yields of fuel gases remain favourably consistent. In contrast, $NiFe_2O_4$ seemed to have inhibited the catalytic performance of the Pt catalysts.

3.2. Effect of Temperature

The effect of operating temperature is critical to different aspects of hydrothermal reforming, such as catalyst performance (reaction selectivity, activity and deactivation), feedstock conversion and/or product selectivity. Figure 3 illustrates the effect of the reaction temperature (250 °C, 300 °C and 350 °C) on the gas products, *CGE* and *HGE* from the hydrothermal reforming of glycerol for 60 min. Experiments were carried out without catalyst and using 1 g of $NiFe_2O_4$ at the different temperature. Evidently, the results demonstrated that $NiFe_2O_4$ increased the selectivity of gas products, *CGE* and *HGE* with

increasing the reaction temperature. At 250 °C, no significant results were observed with and without catalyst, however, on increasing the temperature the gas yields, *CGE* and *HGE* increased substantially as shown in Figure 3.

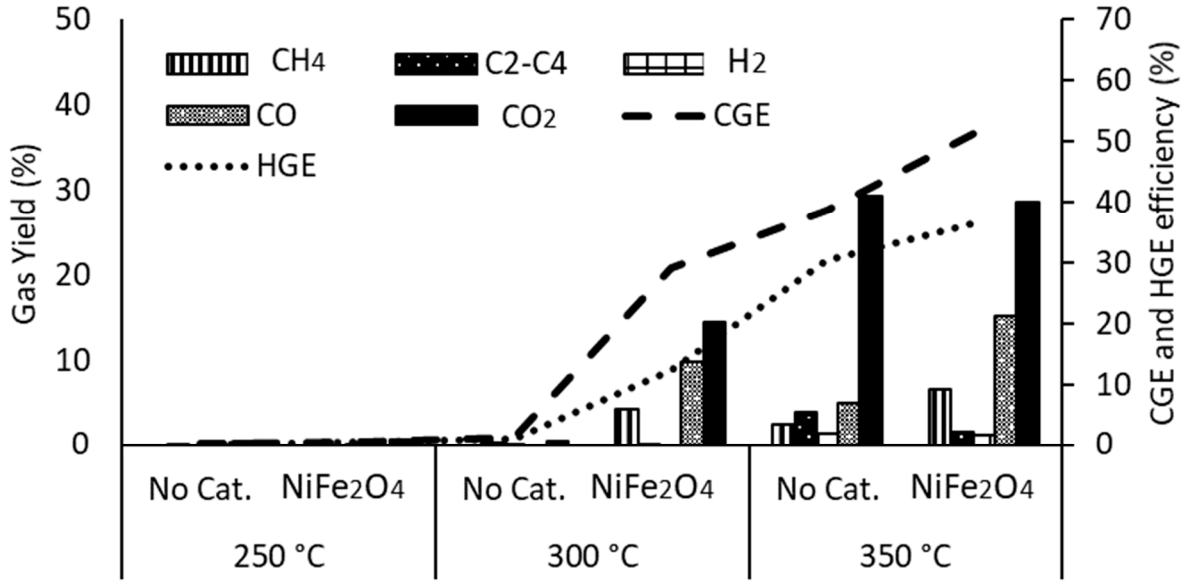

Figure 3. Effect of temperature on catalytic reforming of glycerol without and with the $NiFe_2O_4$ catalyst.

At 300 °C, the $NiFe_2O_4$ showed high gas yields of methane (4.22%), carbon monoxide (9.86%) and carbon dioxide (14.44%). Moreover, at this temperature, the carbon and hydrogen gasification efficiencies increased from 1.20% to 29.12% for *CGE* and from 0.96% to 12.34% for *HGE*, using no catalyst and $NiFe_2O_4$, respectively. However, the most significant results occurred at 350 °C as both tests (with and without catalyst) were selective for all gas products. $NiFe_2O_4$ demonstrated more selectivity at this temperature for CH_4, CO and CO_2, with 6.48%, 15.13% and 28.65%, respectively, in the gas products. Moreover, by increasing the temperature from 300 °C to 350 °C, the *CGE* increased from 29.12% to 52.16% while the *HGE* increased from 30.33% to 36.80%.

Figure 4 shows the effect of the reaction temperature (250, 300 and 350 °C) on the gas products, and carbon and hydrogen gasification efficiencies using 1 g of Ni-Cu/Al_2O_3. The results showed that Ni-Cu/Al_2O_3 catalyst significantly increased the production of gas products, *CGE* and *HGE* when the temperature was increased to 350 °C. At 250 °C, no substantial marks were observed with and without catalyst, however, the gas yields, *CGE* and *HGE* increased substantially increasing the temperature as shown in Figure 4.

At 300 °C, Ni-Cu/Al_2O_3 produced methane (0.13%), C_2–C_4 (0.24%), hydrogen (1.12%), carbon monoxide (0.17%) and carbon dioxide (12.58%). Gasification efficiency increased from 1.20% to 9.71% for *CGE* and from 0.96% to 13.74% for *HGE*, using no catalyst and Ni-Cu/Al_2O_3, respectively. The most significant results were obtained at 350 °C for all experiments, with and without catalysts in terms of gas product yields, *CGE* and *HGE*. The Ni-Cu/Al_2O_3 proved to be selective for CH_4, C_2–C_4, H_2, CO and CO_2, with 3.62%, 7.01%, 2.53%, 6.91% and 43.37% of gas yields, respectively, indicating that this catalyst could be improved to produce further C_2–C_4 gases and H_2, due to its activity for high gas production. Additionally, by increasing the temperature from 300 °C to 350 °C, the *CGE* increased from 9.71% to 59.38% while *HGE* increased from 13.74% to 54.01%.

Figure 5 presents the effect the different Pt-based catalysts (5% Pt/C, 5% Pt/Al_2O_3 and 5% Pt/SiO_2) have on the gas products, carbon and hydrogen gasification efficiencies at a reaction temperature (350 °C). According to the literature, these catalysts are the most reported for reforming reactions to produce hydrogen. Pt-based catalysts supported on solid basic oxides exhibited excellent activity in aqueous-phase reforming [30] and most of

the publications on this reaction type are focused on Pt supported on alumina, due to the high selectivity to H_2 [14,29,31]. However, γ-Al_2O_3 has shown limited stability under these reaction conditions [29,31] and the activity of catalysts supported on alumina becomes mostly poor when compared with those using other supports such as carbon materials [32]. Carbon materials have drawn attention as attractive supports in aqueous-phase reforming due to their high reaction stability. Hence, this could explain why the alumina and carbon supported Pt catalysts were more effective in producing methane and CO than the Pt/SiO_2 catalyst in this present study.

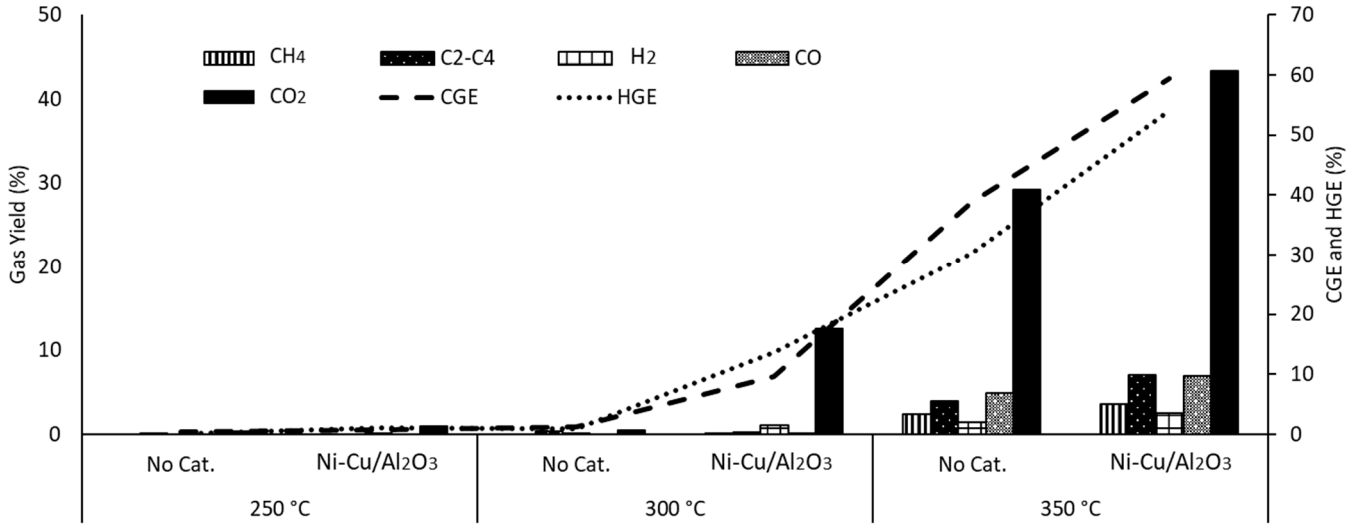

Figure 4. Effect of temperature on catalytic reforming of glycerol without and with the Ni-Cu/Al_2O_3 catalyst.

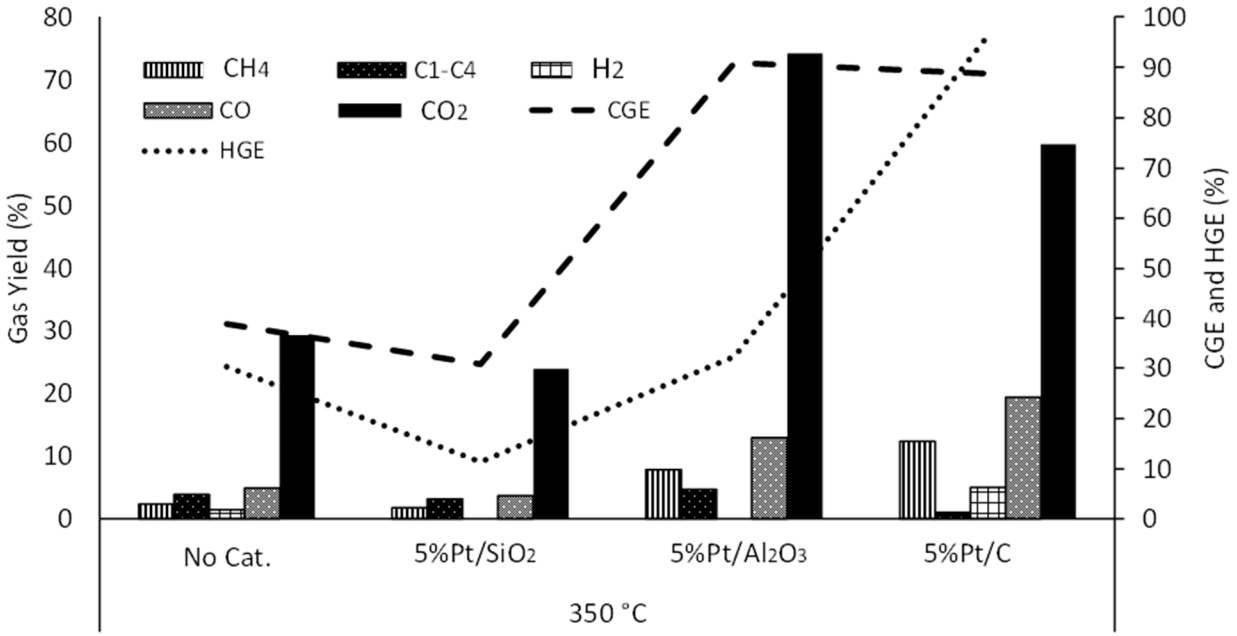

Figure 5. Effect of temperature on catalytic reforming of glycerol without and with the Pt-based catalysts.

Looking at Figure 6, the results agree with the literature in terms of reasonable gas products selectivity, especially using Pt/C at 350 °C with 12.38% of CH_4, 1.1% of C_2–C_4, 5.06% of H_2, 19.39% of CO, 59.74% of CO_2. In addition, 88.8% *CGE* and 96.26% *HGE* were achieved, showing the effectiveness of platinum-based catalysts in organic chemical

reactions in hydrothermal media [33]. Results in Figure 6 clearly show that combining Ni-Cu/Al_2O_3 catalysts with Pt/C and Pt/Al_2O_3 at 350 °C, led to the nearly complete conversion of glycerol, while promoting the formation of methane and CO. Little or no hydrogen gas was found in the gas products from these reactions at 350 °C, instead the yields of methane and CO were enhanced. A similar result can be seen in Figure 7, when NiF_2O_4 was also combined with the Pt/C at 350 °C. However, the combinations of $NiFe_2O_4$ with Pt/Al_2O_3 and Pt/SiO_2 under identical reaction conditions gave poorer or similar results compared to the experiment without catalysts. The formation of these gases, even the presence of large amounts of water in the reactor must mean that the catalytic reaction conditions enhanced both methanation ($CO_2 + 4H_2 \rightarrow CH_4 + 2H_2O$) and reverse water-gas shift reaction ($CO_2 + H_2 \rightarrow CO + H_2O$). Most reports in the literature on the APR of glycerol have targeted hydrogen as the main gaseous product [24,25]. In addition, the conversion of glycerol to methane has been reported but on during gas phase reactions [26]. For instance, Imai et al. [26] carried out gas phase reaction of glycerol and low temperatures favoured CO and H_2 yields, while high temperatures of up to 400 °C, favoured methane production via CO methanation. In contrast, this present work showed that methanation occurred at 350 °C, with complete consumption of hydrogen, leaving a significant amount of CO in the gas product.

3.3. Structural Stability of Used Catalysts in Hydrothermal Media

XRD measurements were performed in fresh and used catalysts to evaluate potential changes in crystalline phases and the presence of reaction-generated impurities in hydrothermal media. Through this structural stability study, the potential of catalyst reuse could be estimated or established, without lengthy experimental re-testing.

3.3.1. $NiFe_2O_4$

The XRD patterns of the fresh and recovered $NiFe_2O_4$ powders are shown in Figure 8 and correspond to the characteristic peaks of the cubic spinel-phase $NiFe_2O_4$ even after being recovered at 250, 300 and 350 °C. Fe_2O_3 and NiO were identified in both recovered samples. The intensity of the $NiFe_2O_4$ spinel peaks increased with temperature, suggesting that the synthesis of $NiFe_2O_4$ continued after the catalytical glycerol reforming reactions and regeneration procedure. It is known that temperature has a strong influence on the purity, size, structural and magnetic properties of materials prepared by the combustion route [27]. Figure 8 shows the presence of graphitic carbon in the fresh $NiFe_2O_4$ catalyst, which must have remained after its synthesis by the combustion method. The used $NiFe_2O_4$ gave similar XRD diffractograms as the fresh catalyst until 350 °C when addition peaks corresponding to coke ($2\theta = 44°, 53°$) were observed. A similar observation was made in our previous work [27] with the same $NiFe_2O_4$ catalyst prepared by the combustion reaction method during the supercritical water gasification (SCWG) of eucalyptus wood chips at 450 and 500 °C for 60 min. After the third reaction cycle, the results demonstrated the formation of coke caused the deactivation of the $NiFe_2O_4$ and consequently led to a 13.6% reduction in H_2 mol% and a 5.6% reduction in biomass conversion.

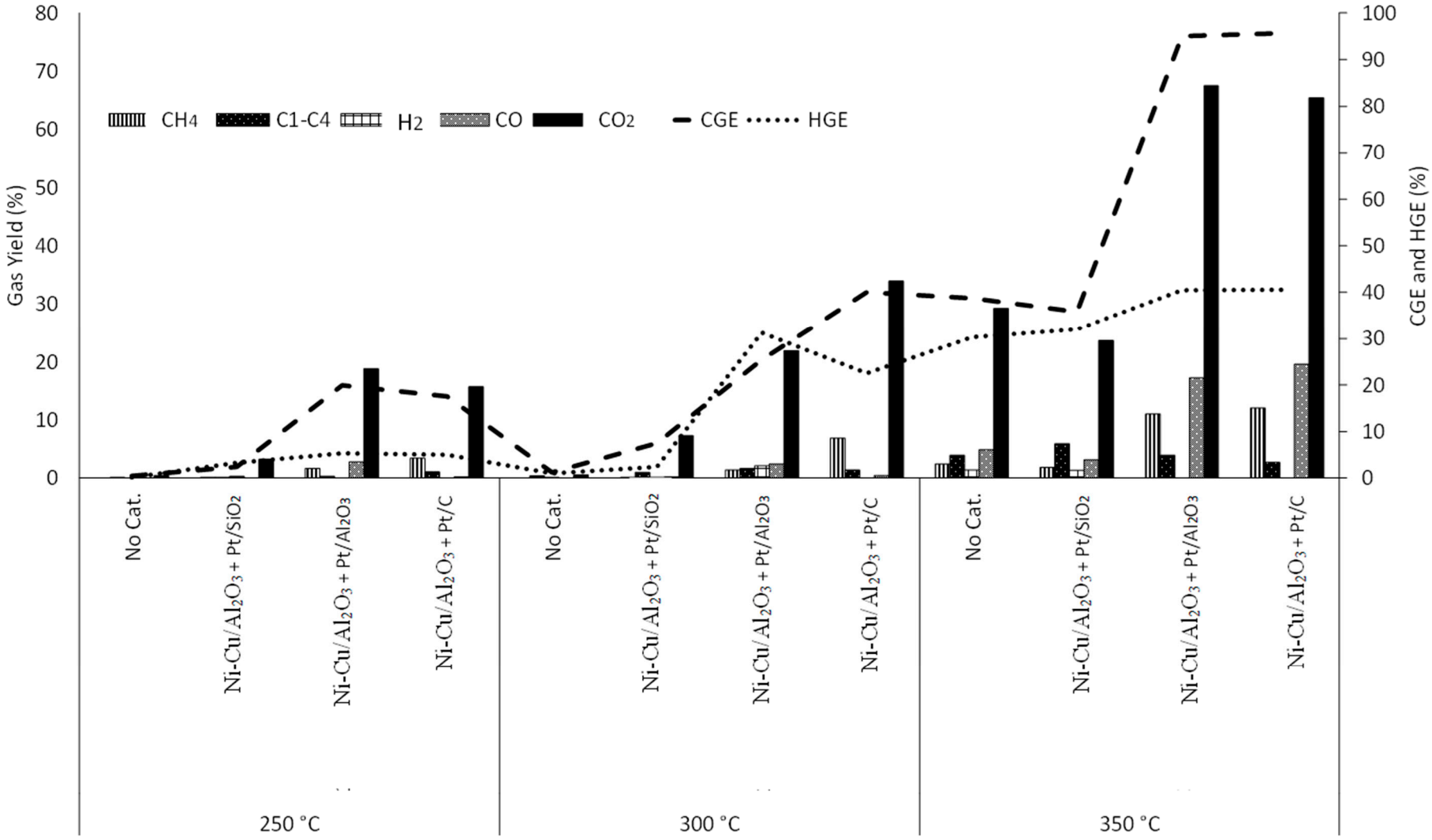

Figure 6. Effect of temperature on reforming of glycerol using 50/50 wt% combination of Ni-Cu/Al_2O_3 and the Pt-based catalysts.

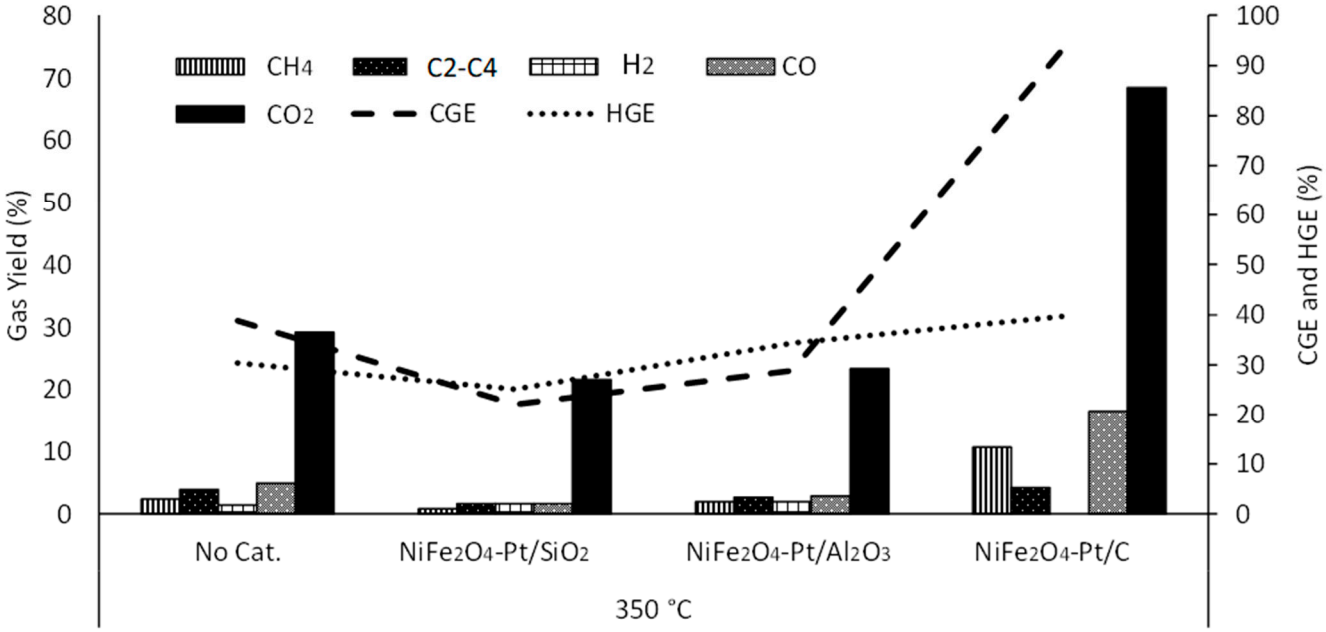

Figure 7. Effect of using 50/50 wt% combination of $NiFe_2O_4$ and the Pt-based catalysts for catalytic reforming of glycerol at 350 °C.

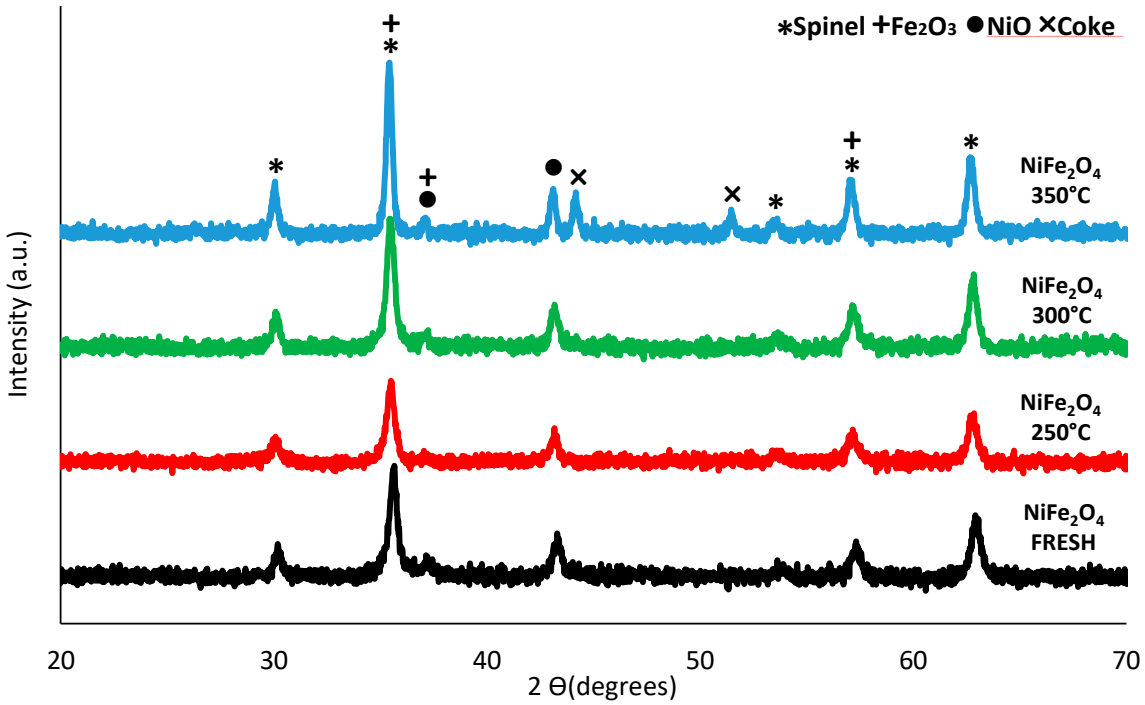

Figure 8. XRD of the fresh and recovered $NiFe_2O_4$.

3.3.2. Physical Mixtures of $NiFe_2O_4$ and Pt Catalysts

Figure 9 shows powder X-ray diffraction (XRD) patterns of fresh $NiFe_2O_4$ and recovered $NiFe_2O_4$-Pt/C, $NiFe_2O_4$-Pt/Al_2O_3 and $NiFe_2O_4$-Pt/SiO_2 at 350 °C. The XRD patterns demonstrated that all peaks corresponding to the recovered combined catalysts were identified and may remain active for reuse.

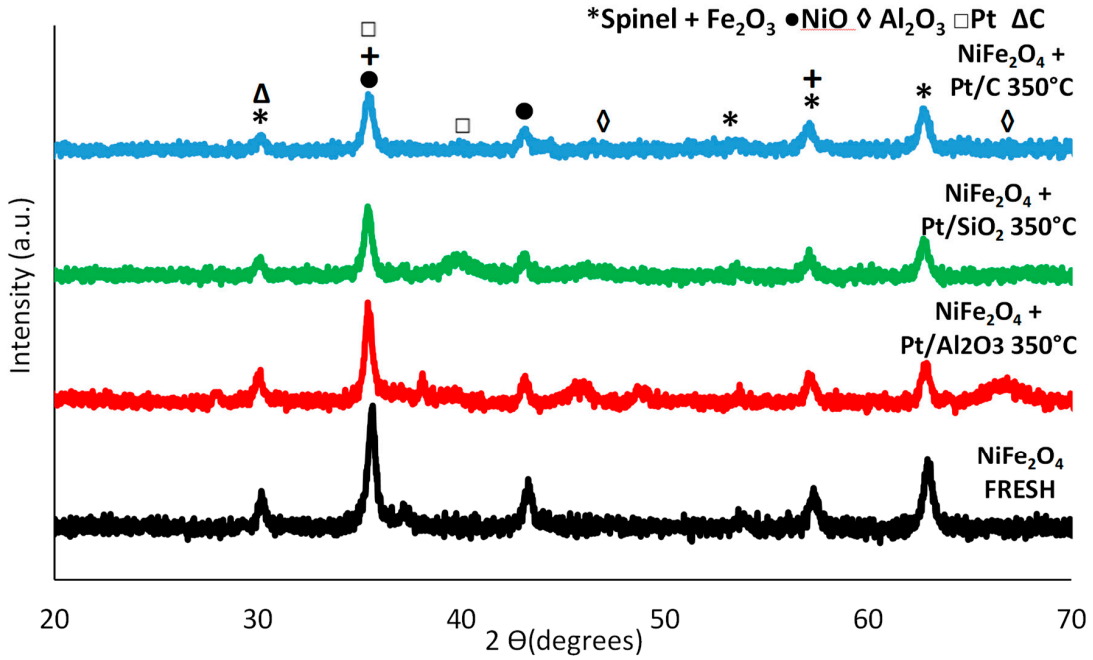

Figure 9. XRD of the fresh and recovered $NiFe_2O_4$-Pt/C, $NiFe_2O_4$-Pt/Al_2O_3 and $NiFe_2O_4$-Pt/SiO_2.

3.3.3. Ni-Cu/Al_2O_3

Figure 10 shows the XRD patterns of the fresh and recovered N-Cu/Al_2O_3 catalyst at 250, 300 and 350 °C. All catalysts show diffraction peaks at 2θ = 37.3°, 45.8° and 67.3° which can be ascribed to the crystalline phase of γ-Al_2O_3. Reflection peaks at 2θ = 37.3°, 43.4°, 63.2°, and 75.3° are assigned to NiO. Peaks of CuO can be confirmed to be the monoclinic phase of CuO. The diffraction peaks of Ni_x–$Cu_{1-x}O$ and NiO are almost overlapped [34].

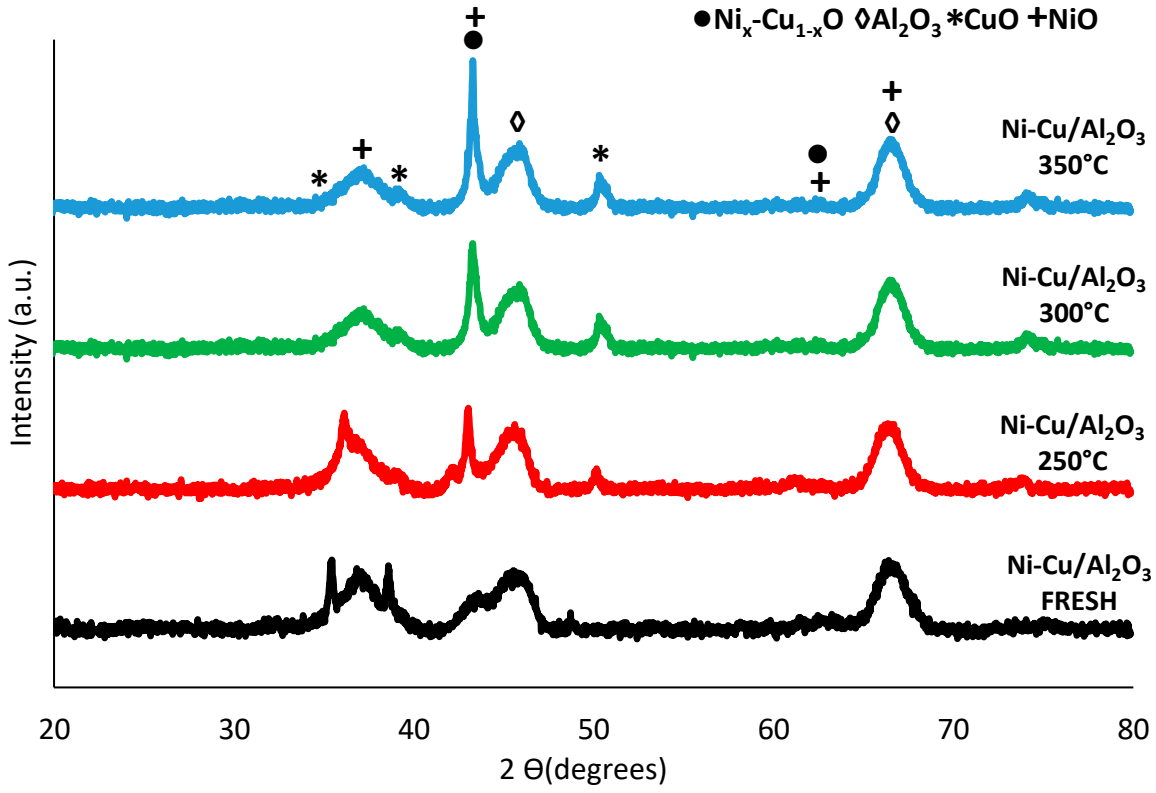

Figure 10. XRD of the fresh and recovered Ni-Cu/Al_2O_3.

Ni-Cu bimetallic catalysts have been reported to have high catalytic activity at relatively lower costs than platinum group metals (PGM). During preparation, Cu and Ni crystallise into a closely packed cubic lattice when they form solid solutions (alloys), making them highly versatile for a range of catalytic reactions including methane dissociation [13], glycerol hydrogenolysis [35] and steam reforming [36]. They have also been applied for reactions involving hydrogenation [37], water–gas shift reactions [38] and alcohol dehydrogenation reactions [39].

3.3.4. Ni-Cu/Al_2O_3-Pt/SiO_2

Figure 11 shows powder X-ray diffraction (XRD) patterns of five series of catalysts: fresh N-Cu/Al_2O_3, fresh Pt/SiO_2 and the recovered combined catalysts Ni-Cu/Al_2O_3-Pt/Silica at 250 °C, 300 °C and 350 °C. The XRD patterns of the Pt/ SiO_2 showed two significant diffraction peaks at 2θ of 39.7° and 46.3°, corresponding to facets of metallic Pt, respectively [40]. It is possible to identify all peaks corresponding to the combining between the two fresh catalysts indicating that the recovered catalyst may remain active for reuse.

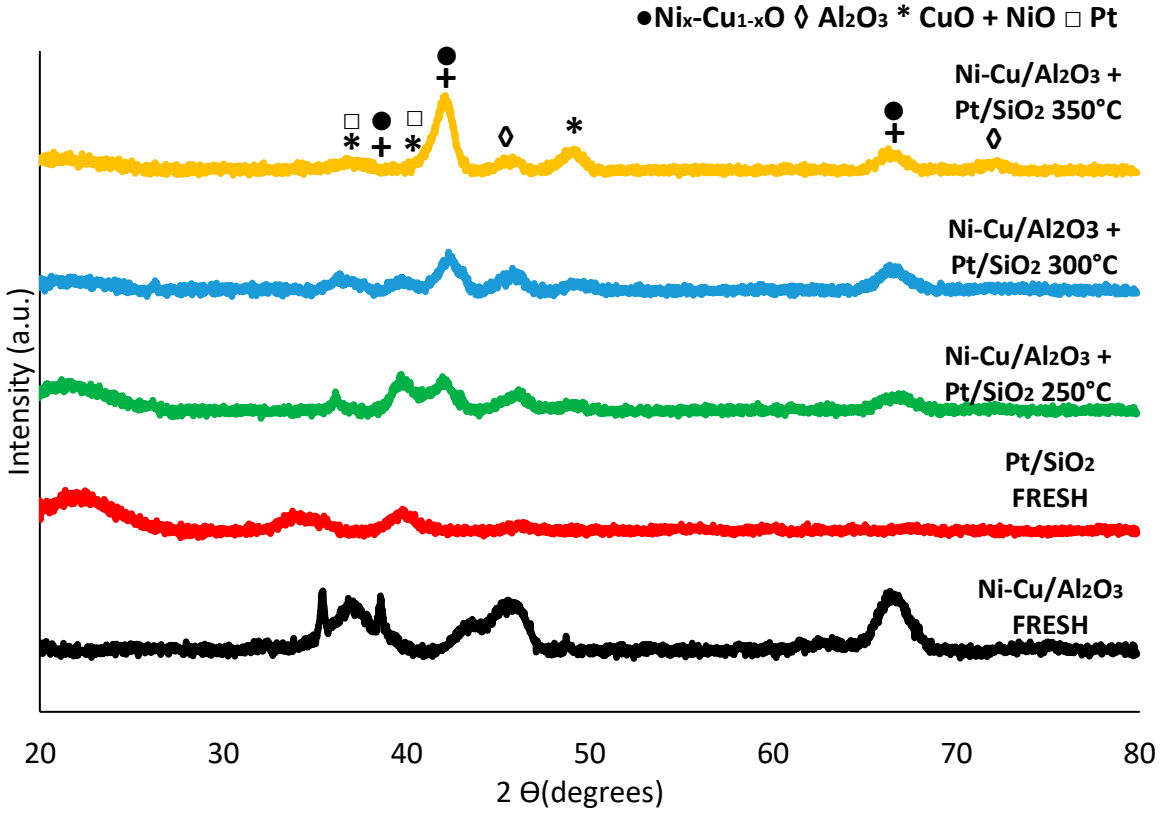

Figure 11. XRD of the fresh and recovered Ni-Cu/Al_2O_3 + Pt/SiO_2.

The effect of different supports (ZrO_2, SiO_2, γ-Al_2O_3 and α-Al_2O_3 modified with Ce and Zr) of the activity of platinum catalysts during SRG was studied by Pompeo, Santori, and Nichio [41], at temperatures below 450 °C. The authors observed the platinum catalysts supported on the acidic ZrO_2, and γ-Al_2O_3 suffered fast deactivation resulting from coke formation. In contrast, the neutral SiO_2 demonstrated good stability and promoted the scission of C-C, O-H and C-H bonds.

3.3.5. Ni-Cu/Al_2O_3-Pt/Al_2O_3

Alumina and silica are among the most investigated catalyst supports used for hydrothermal reforming of glycerol [36], alumina and silica are the most investigated materials. These supports may change their crystalline phases under hydrothermal conditions, which may alter their properties e.g., acidity. For instance, Cifcti et al. (2014) investigated the catalytic activity of Pt supported on silica, γ-alumina, and amorphous silica–alumina with different Al contents for hydrothermal reforming of glycerol [25]. The authors reported that the Al-containing supports formed boehmite after extended reaction times, which led to surface acidity. This led to increased yields of hydroxyacetone and 1,2-propanediol via the promotion of glycerol dehydration and hydrogenation, respectively [25].

Based on these results, the selectivity of the reaction process may be affected by the interaction between the support and the active phase, so that hydrogen spillover from Pt to alumina can lead to a higher concentration of alkanes in the products [9]. Figure 12 presents that XRD patterns for a series of the 50/50 wt% combination of Ni-Cu/Al_2O_3 and Pt/Al_2O_3 catalysts. It is the first time to our knowledge that this type of catalyst combination is being reported in the literature for hydrothermal reforming of glycerol reactions.

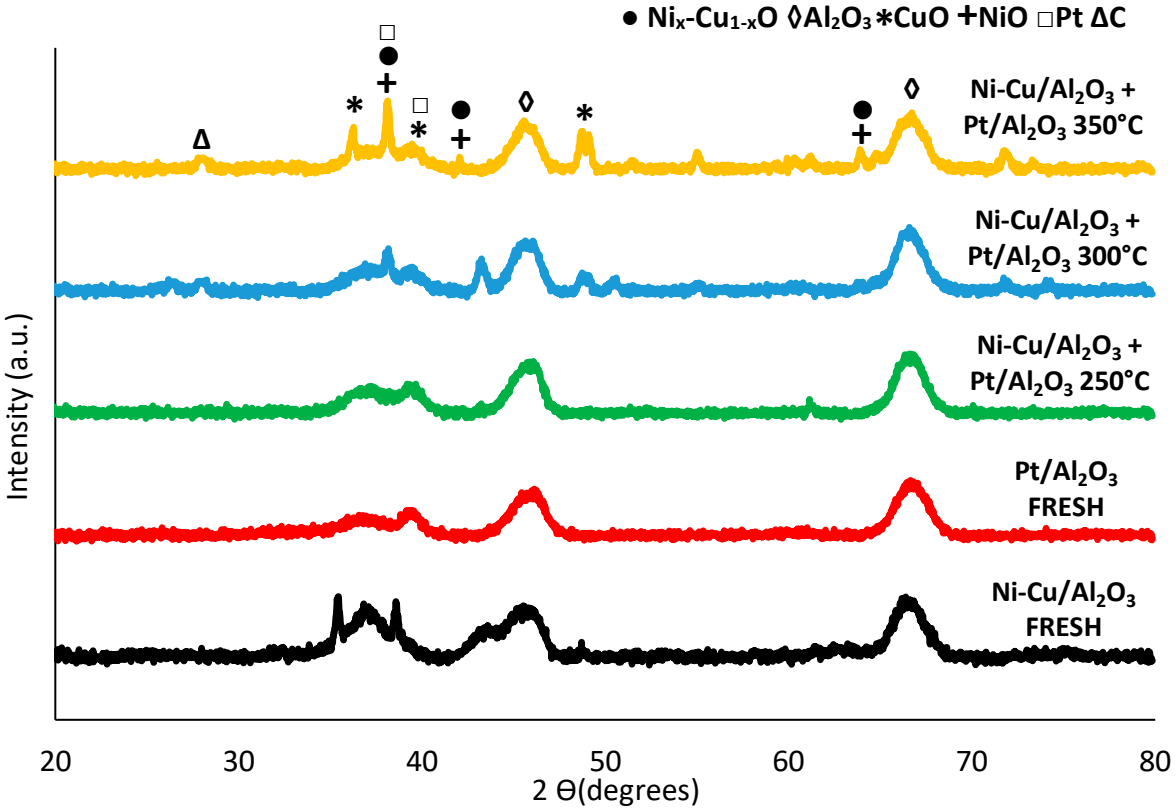

Figure 12. XRD of the fresh and recovered Ni-Cu/Al_2O_3 + Pt/Al_2O_3.

3.3.6. Ni-Cu/Al_2O_3-Pt/C

Carbon-based supports are a valid alternative to inorganic oxides for developing an active catalyst. The XRD patterns obtained for the fresh 5% Pt/C, fresh Ni-Cu/Al_2O_3 and for the recovered catalysts are shown in Figure 13. As demonstrated the XRD of Pt/C showed four obvious peaks. A broad peak at 2θ of 25.01° indicated the graphite structure of the carbon support. The other three peaks appeared at a 2θ of 39.58°, 46.04° and 67.09° represented the characteristic diffraction peaks of Platinum, respectively. The recovered catalysts samples demonstrated to be in agreement with the combination between fresh catalysts and increasing the intensity of each peak with increasing temperature reaction.

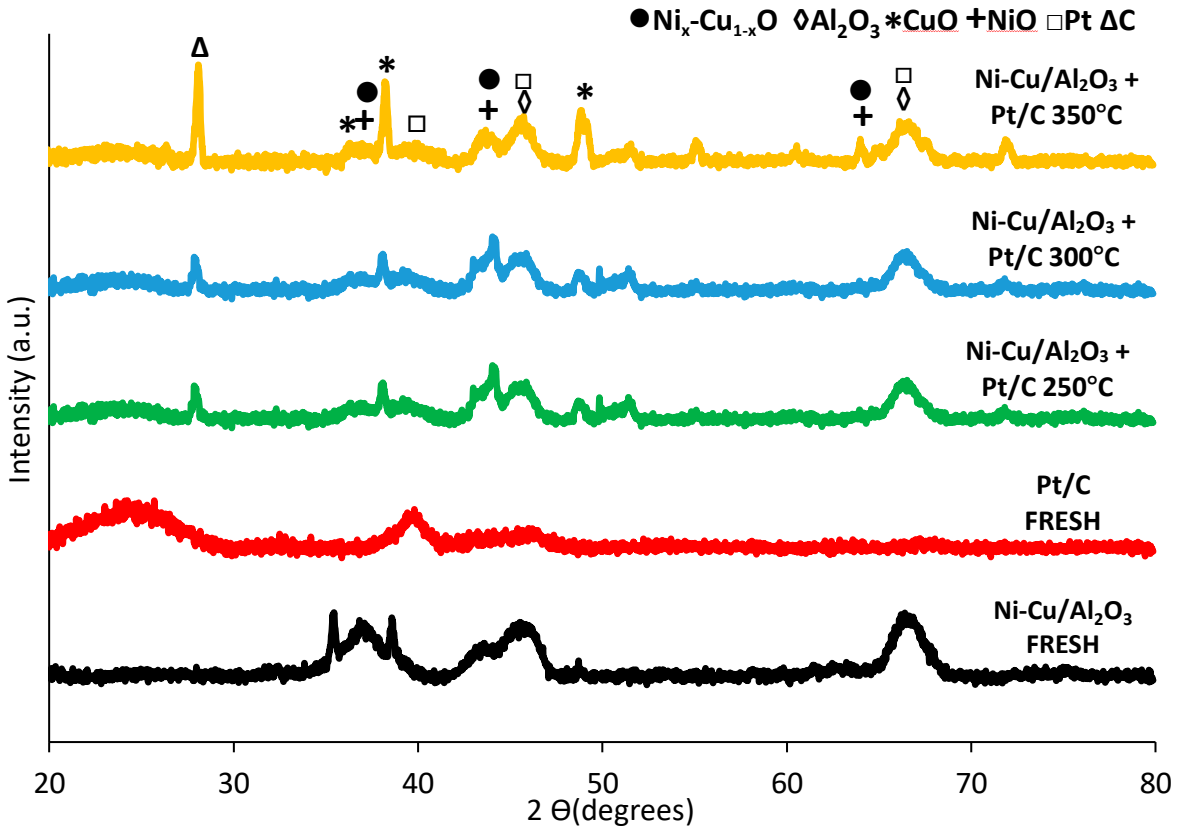

Figure 13. XRD of the fresh and recovered Ni-Cu/Al_2O_3-Pt/C.

3.3.7. Catalyst Reuse

To evaluate the catalyst recyclability one test was performed using the recovered Pt/Al_2O_3 from the reaction carried out at 350 °C, which gave the highest glycerol conversion during first use. The results obtained were compared to the fresh catalyst tested and found to be very similar. In the presence of the reused Pt/Al_2O_3 catalyst 99.56% glycerol conversion was obtained, with *CGE* and *HGE* of 89.81% and 31.61% respectively. These values are similar to those obtained with the fresh catalyst, which gave 99.84% glycerol conversion, 90.93% *CGE* and 32.27% *HGE*. Figure 14 compares the XRD patterns for the fresh Pt/Al_2O_3, recovered Pt/Al_2O_3 after first reaction at 350 °C (1st cycle) and recovered Pt/Al_2O_3 catalyst after second reaction at 350 °C (2nd cycle). Up to the second cycle tested in this work, the recovered Pt/Al_2O_3 showed similar XRD patterns and activity as the fresh catalyst, indicating that it could remain active for more cycles of catalytic reforming of glycerol. The next set of work will extensively test each promising catalyst systems over four cycles to evaluate their stability during glycerol reforming reactions under the same sets of conditions.

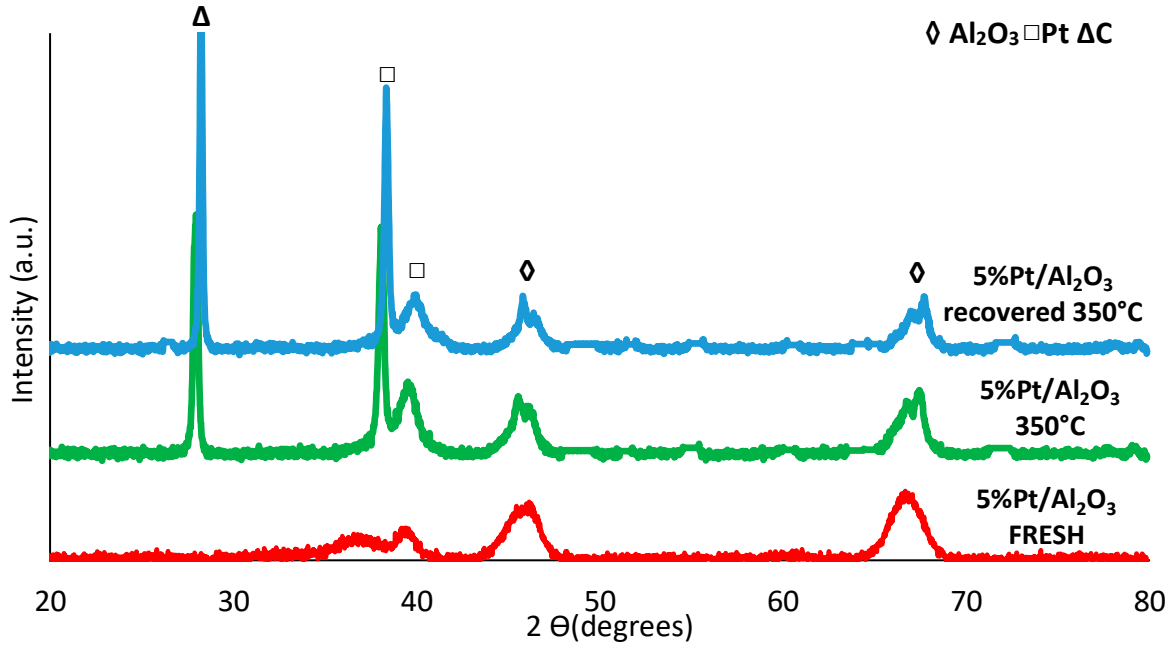

Figure 14. XRD of the fresh, tested (1st cycle) and recovered (2nd cycle) Pt/Al_2O_3.

4. Conclusions

Various heterogeneous catalysts and their physical mixtures ($NiFe_2O_4$ $Ni\text{-}Cu/Al_2O_3$, Pt/C, $Ni\text{-}Cu/Al_2O_3\text{-}Pt/C$, $Ni\text{-}Cu/Al_2O_3\text{-}Pt/Al_2O_3$ and $Ni\text{-}Cu/Al_2O_3\text{-}Pt/SiO_2$) have been screened for the hydrothermal reforming of glycerol at 250 °C, 300 °C and 350 °C for reaction times of 60 min. While CO_2 remained the most dominant gas product, the best catalyst to obtain high glycerol conversion and selectivity towards fuel gases was the 1:1 mass ratio combination of $Ni\text{-}Cu/Al_2O_3$ and Pt/C at 350 °C. This combined catalyst gave good activity and selectivity for methane, hydrocarbon gases, carbon monoxide, carbon gasification efficiency and hydrogen gasification efficiency. Besides, the Pt/C gave the highest hydrogen yield but, the combined 1:1 $Ni\text{-}Cu/Al_2O_3$ and Pt/C catalyst may be more cost-effective in terms of lowering catalyst cost to achieve a similar result as Pt/C alone. The recovered catalysts showed similar XRD patterns indicating that they could remain active for more cycles of catalytic reforming of glycerol. Preliminary reforming tests with recovered Pt/Al_2O_3 showed consistent glycerol conversion and gas yields at 350 °C. The obtained results provide a good background for the synthesis of reforming and water-gas shift multi-metallic catalysts and nano-catalysts for tuning the selectivity of fuel gas products as appropriate, which is the next stage of this research.

Author Contributions: Conceptualization, C.T.A. and J.A.O.; methodology, C.T.A. and J.A.O.; formal analysis, C.T.A. and J.A.O.; investigation, C.T.A. and J.A.O.; resources, C.T.A. and J.A.O.; writing—original draft preparation, C.T.A. and J.A.O.; writing—review and editing, C.T.A. and J.A.O.; supervision, C.T.A. and J.A.O. All authors have read and agreed to the published version of the manuscript.

Funding: This work was supported by the Marie Curie Fellowship, Grant Number 892998 for C.T.A. and the Biomass Biorefinery Network (BBNet), a BBSRC/EPSRC funded Network in Industrial Biotechnology and Bioenergy (BBSRC NIBB), Grant Number BB/S009779/1 for J.A.O.

Institutional Review Board Statement: Not applicable.

Informed Consent Statement: Not applicable.

Data Availability Statement: Not applicable. All relevant data presented in this paper.

Acknowledgments: The authors would like to thank the Energy & Bioproducts Research Institute (EBRI) and Aston University, UK, for all support received.

Conflicts of Interest: The authors declare no conflict of interest. The funders had no role in the design of the study; in the collection, analyses, or interpretation of data; in the writing of the manuscript, or in the decision to publish the results.

References

1. Huang, K.; Peng, X.; Kong, L.; Wu, W.; Chen, Y.; Maravelias, C.T. Greenhouse Gas Emission Mitigation Potential of Chemicals Produced from Biomass. *ACS Sust. Chem. Eng.* **2021**, *9*, 14480–14487. [CrossRef]
2. Wang, K.; Zuo, Y.; Pei, P.; Xie, X.; Wei, M.; Xiong, J.; Zhang, P. Highly efficient hydrogen production via a zinc carbon @ nickel system. *Int. J. Hydrog. Energy* **2022**, *47*, 5354–5360. [CrossRef]
3. Ballantyne, A.P.; Alden, C.B.; Miller, J.B.; Tans, P.P.; White, J.W.C. Increase in observed net carbon dioxide uptake by land and oceans during the past 50 years. *Nature* **2012**, *488*, 70–72. [CrossRef] [PubMed]
4. Hermann, B.G.; Blok, K.; Patel, M.K. Producing Bio-Based Bulk Chemicals Using Industrial Biotechnology Saves Energy and Combats Climate Change. *Environ. Sci. Technol.* **2007**, *41*, 7915–7921. [CrossRef] [PubMed]
5. Ardi, M.S.; Aroua, M.K.; Hashim, A.N. Progress, prospect and challenges in glycerol purification process: A review. *Renew. Sust. Energy Rev.* **2015**, *42*, 1164–1173. [CrossRef]
6. Yahya, M.; Dutta, A.; Bouri, E.; Wadström, C.; Uddin, G.S. Dependence structure between the international crude oil market and the European markets of biodiesel and rapeseed oil. *Renew. Energy* **2022**, *197*, 594–605. [CrossRef]
7. Sittijunda, S.; Reungsang, A. Valorization of crude glycerol into hydrogen, 1,3-propanediol, and ethanol in an up-flow anaerobic sludge blanket (UASB) reactor under thermophilic conditions. *Renew. Energy* **2020**, *161*, 361–372. [CrossRef]
8. Zhang, J.; Wang, Y.; Muldoon, V.L.; Deng, S. Crude glycerol and glycerol as fuels and fuel additives in combustion applications. *Renew. Sust. Energy Rev.* **2022**, *159*, 112206. [CrossRef]
9. Fasolini, A.; Cespi, D.; Tabanelli, T.; Cucciniello, R.; Cavani, F. Hydrogen from Renewables: A Case Study of Glycerol Reforming. *Catalysts* **2019**, *9*, 722. [CrossRef]
10. Sahraei, A.; Desgagnés, O.; Larachi, A.F.; Iliuta, M.C. Ni-Fe catalyst derived from mixed oxides Fe/Mg-bearing metallurgical waste for hydrogen production by steam reforming of biodiesel by-product: Investigation of catalyst synthesis parameters and temperature dependency of the reaction network. *Appl. Catal. B Environ.* **2020**, *279*, 119330. [CrossRef]
11. Yun, S.; Zhang, Y.; Zhang, L.; Liu, Z.; Deng, Y. Ni and Fe nanoparticles, alloy and Ni/Fe-Nx coordination co-boost the catalytic activity of the carbon-based catalyst for triiodide reduction and hydrogen evolution reaction. *J. Coll. Int. Sci.* **2022**, *615*, 501–516. [CrossRef] [PubMed]
12. Chakinala, A.G.; Chinthaginjala, J.K.; Seshanb, K.; van Swaaij, W.P.M.; Kersten, S.R.A.; Brilman, D.W.F. Catalyst screening for the hydrothermal gasification of aqueous phase of bio-oil. *Catal. Today* **2012**, *195*, 83–92. [CrossRef]
13. Seretis, A.; Tsiakaras, P. A thermodynamic analysis of hydrogen production via aqueous phase reforming of glycerol. *Fuel Process. Technol.* **2015**, *134*, 107–115. [CrossRef]
14. Shabaker, J.W.; Huber, G.W.; Davda, R.R.; Cortright, R.D.; Dumesic, J.A. Aqueous phase reforming of ethylene glycol over supported platinum catalysts. *Catal. Lett.* **2003**, *88*, 1–8. [CrossRef]
15. Liguras, D.K.; Kondarides, D.I.; Verykios, X.E. Production of hydrogen for fuel cells by steam reforming of ethanol over supported noble metal catalysts. *Appl. Catal. B Environ.* **2003**, *43*, 345–354. [CrossRef]
16. Roslan, N.A.; Abidin, S.Z.; Osazuwa, O.U.; Chin, S.Y.; Taufiq-Yap, Y.H. Enhanced syngas production from glycerol dry reforming over Ru promoted -Ni catalyst supported on extracted Al_2O_3. *Fuel* **2022**, *314*, 123050. [CrossRef]
17. Roslan, N.A.; Abidin, S.Z.; Ideris, A.; Vo, D.V.N. A review on glycerol reforming processes over Ni-based catalyst for hydrogen and syngas productions. *Int. J. Hydrog. Energy* **2020**, *45*, 18466–18489. [CrossRef]
18. Demsash, H.D.; Kondamudi, K.V.K.; Upadhyayula, S.; Mohan, R. Ruthenium doped nickel-alumina-ceria catalyst in glycerol steam reforming. *Fuel Proc. Technol.* **2018**, *169*, 150–156. [CrossRef]
19. Suffredini, D.F.P.; Thyssen, V.V.; de Almeida, P.M.M.; Gomes, R.S.; Borges, M.C.; de Farias, A.M.D.; Assaf, E.M.; Fraga, M.A.; Brandão, S.T. Renewable hydrogen from glycerol reforming over nickel aluminate-based catalysts. *Catal. Today* **2017**, *289*, 96–104. [CrossRef]
20. Yang, T.; Wang, P.; Li, Q.; Xia, C.; Yin, F.; Liang, C.; Zhang, Y. Hydrogen absorption and desorption behavior of Ni catalyzed MgeYeCeNi nanocomposites. *Energy* **2018**, *165*, 709–719. [CrossRef]
21. Jiao, Y.; He, Z.; Wang, J.; Chen, Y. n-decane steam reforming for hydrogen production over mono- and bi-metallic Co-Ni/Ce-Al2O3 catalysts: Structure-activity correlations. *Energy Conv. Manag.* **2017**, *148*, 954–962. [CrossRef]
22. Touri, A.E.; Taghizadeh, M. Hydrogen Production via Glycerol Reforming over Pt/SiO2 Nanocatalyst in a Spiral-Shaped Microchannel Reactor. *Int. J. Chem. Reactor Eng.* **2016**, *14*, 1059–1068. [CrossRef]
23. Chakinala, N.; Chakinala, A.G. Catalytic reforming of glycerol in hot compressed water: Role of metal and support. *J. Sup. Fluids* **2022**, *180*, 105459. [CrossRef]
24. Boga, D.A.; Liu, F.; Bruijnincx, P.C.A.; Weckhuysen, B.M. Aqueous-phase reforming of crude glycerol: Effect of impurities on hydrogen production. *Catal. Sci. Technol.* **2016**, *6*, 134–143. [CrossRef]
25. Ciftci, A.; Ligthart, M.D.A.J.; Arno, A.O.S.; van Hoof, J.F.; Friedrich, H.; Emiel Hensen, J.M. Pt-Re synergy in aqueous-phase reforming of glycerol and the water–gas shift reaction, Pt-Re synergy in aqueous-phase reforming of glycerol and the water–gas shift reaction. *J. Catal.* **2014**, *311*, 88–101. [CrossRef]

26. Imai, H.; Yamawaki, M.; Li, X. Direct Synthesis of Methane from Glycerol by Using Silica-modified Nickel Catalyst. *J. Jpn. Petrol.* **2017**, *60*, 311–321. [CrossRef]
27. Borges, A.C.P.; Onwudili, J.A.; Andrade, H.; Alves, C.; Ingram, A.; Vieira de Melo, S.; Torres, E. Catalytic Properties and Recycling of $NiFe_2O_4$ Catalyst for Hydrogen Production by Supercritical Water Gasification of Eucalyptus Wood Chips. *Energies* **2020**, *13*, 4553. [CrossRef]
28. Gao, N.; Salisu, J.; Quan, C.; Williams, P. Modified nickel-based catalysts for improved steam reforming of biomass tar: A critical review. *Renew. Sust. Energy Rev.* **2021**, *145*, 111023. [CrossRef]
29. Luo, M.F.; Lin, W.R.; Wen, W.H.; Chang, B.W. Methanol electro-oxidation and induced sintering on Pt nanoclusters supported on thin-film Al_2O_3/NiAl(1 0 0). *Surf. Sci.* **2008**, *602*, 3258–3265. [CrossRef]
30. Guo, Y.; Liu, X.; Azmat, M.U.; Xu, W.; Ren, J.; Wang, Y.; Lu, G. Hydrogen production by aqueous-phase reforming of glycerol over Ni-B catalysts. *Int. J. Hydrog. Energy* **2012**, *37*, 227–234. [CrossRef]
31. Koichumanova, K.; Vikla, A.K.K.; de Vlieger, D.J.M.; Seshan, K.; Mojet, B.L.; Lefferts, L. Towards stable catalysts for aqueous phase conversion of ethylene glycol for renewable hydrogen. *Chem. Sus. Chem.* **2013**, *6*, 1717–1723. [CrossRef]
32. Kim, T.; Song, H.; Heechul, K.; Jong, Y.; Chung, S. Steam reforming of n-dodecane over K2Ti2O5-added Ni-alumina and Ni-zirconia (YSZ) catalysts. *Int. J. Hydrog. Energy* **2016**, *41*, 17922–17932. [CrossRef]
33. Razaq, I.; Simons, K.E.; Onwudili, J.A. Parametric Study of Pt/C-Catalysed Hydrothermal Decarboxylation of Butyric Acid as a Potential Route for Biopropane Production. *Energies* **2021**, *14*, 3316. [CrossRef]
34. Tribalis, A.; Tsilomekis, G.; Boghosian, S. Molecular structure and reactivity of titania-supported transition metal oxide catalysts synthesized by equilibrium deposition filtration for the oxidative dehydrogenation of ethane. *Comptes Rendus Chimie* **2016**, *19*, 1226–1236. [CrossRef]
35. Torres, A.; Roy, D.; Subramaniam, B.; Chaudhari, R.V. Kinetic Modeling of Aqueous-Phase Glycerol Hydrogenolysis in a Batch Slurry Reactor. *Ind. Eng. Chem. Res.* **2010**, *49*, 10826–10835. [CrossRef]
36. Adeniyi, A.G.; Ighalo, J.O. Hydrogen production by the steam reforming of waste lubricating oil. *Ind. Chem Eng.* **2019**, *61*, 403–414. [CrossRef]
37. Vasiliadou, E.S.; Eggenhuisen, T.M.; Munnik, P.; de Jongh, P.E.; de Jong, K.P.; Lemonidou, A.A. Synthesis and performance of highly dispersed Cu/SiO2 catalysts for the hydrogenolysis of glycerol. *Appl. Catal. B Environ.* **2014**, *145*, 108–119. [CrossRef]
38. Schwengber, C.A.; Silva, F.A.; Schaffner, R.A.; Fernandes-Machado, N.R.C.; Ferracin, R.J.F.; Bach, V.R.; Alves, H.J. Methane dry reforming using Ni/Al2O3 catalysts: Evaluation of the effects of temperature, space velocity and reaction time. *J. Environ. Chem. Eng.* **2016**, *4*, 3688–3695. [CrossRef]
39. Wu, H.; Guo, Y.Y.; Jiang, X.; Qi, Y.; Sun, B.; Li, H.; Zheng, J.; Li, X. A rare earth hydride supported ruthenium catalyst for the hydrogenation of N-heterocycles: Boosting the activity via a new hydrogen transfer path and controlling the stereoselectivity. *Chem. Sci.* **2019**, *10*, 10459–10465. [CrossRef]
40. Deng, L.; Zhou, Z.; Shishido, T. Behavior of active species on Pt-Sn/SiO2 catalyst during the dehydrogenation of propane and regeneration. *Appl. Catal. A Gen.* **2020**, *606*, 117826. [CrossRef]
41. Pompeo, F.; Santori, G.; Nichio, N.N. Hydrogen and/or syngas from steam reforming of glycerol. Study of platinum catalysts. *Int. J. Hydrog. Energy* **2010**, *35*, 8912–8920. [CrossRef]